Structural Eng./Earthquake Eng., JSCE, Vol. 14, No. 2, 129s—138s, 1997 July
(J. Struct. Mech. Earthquake Eng., JSCE, No. 570/ I —40)

SEISMIC WAVE AMPLIFICATION DUE TO TOPOGRAPHY AND GEOLOGY IN KOBE DURING HYOGO-KEN NANBU EARTHQUAKE

Hirokazu TAKEMIYA[1] and Maher ADAM[2]

[1]Member of JSCE, Dr. of Eng., Professor, Dept. of Environmental and Civil Eng, Okayama University, (Tsushima-Naka, 3-1-1, Okayama, 700, Japan)

[2]Member of JSCE, M. Eng., Ph.D. Candidate, Graduate School of Science and Technology, Okayama University

The Hyogo-ken Nanbu Earthquake, 17 January 1995 caused by inland active faults resulted in a disaster belt zone of JMA intensity VII in Kobe city. In this paper, addressing attention to the geological features, the authors conducted computer simulation in order to interpret the above consequence. The gradually increasing surface alluvium toward the coast and the deep Osaka Group soils bounded by abrupt dipping of the rock formation at the foot of Rokko range are focused. The results shows that the former is related to the localized amplification of the short period motions (0.5 - 1s) while the latter to the long period motions (1 - 2s) and that the seismic amplification in alluvium might be more concerned with the heavy damage.

Key Words : Hyogo-ken Nanbu earthquake, disaster belt, site amplification, deep diluvium, shallow alluvium, seismic wave propagation, time domain analysis

1. INTRODUCTION

The Hyogo-ken Nanbu Earthquake, of magnitude 7.2 on the Richter scale hit Kobe and other parts of Kinki area of Japan on 17 January 1995, leading to one of the worst disaster to hit Japan. The damage of intensity VII on the Japan Meteorological Agency (JMA) scale was concentrated in a narrow zone of 1 - 1.5 km width, bounded by the Japan Railway line in the north and the Hanshin Expressway Kobe line in the south, stretched over 25 Km in the east-west direction along the Kobe coast as indicated in **Fig.1** that is called "Seismic disaster belt". The details have been reported elsewhere[1].

First, seismologists suspected existence of an active fault just beneath the seismic disaster belt zone. The aftershock observation was conducted immediately after the main shock. Those locations are marked in **Fig.1**[2]. It is noted that these locations are shifted about 1 km to the north from the disaster belt zone toward the Rokko range. This shift and the evidence of no aftershock sources at the later left an essential scientific puzzle to seismologists and earthquake engineers how such a devastating seismic action was generated.

Overlapping of the damage area of intensity VII on the isobath lines of supporting soil whose N-value is more than 50 or the equivalent, revealed the effect of surface soft soils. Within the disaster belt zone,

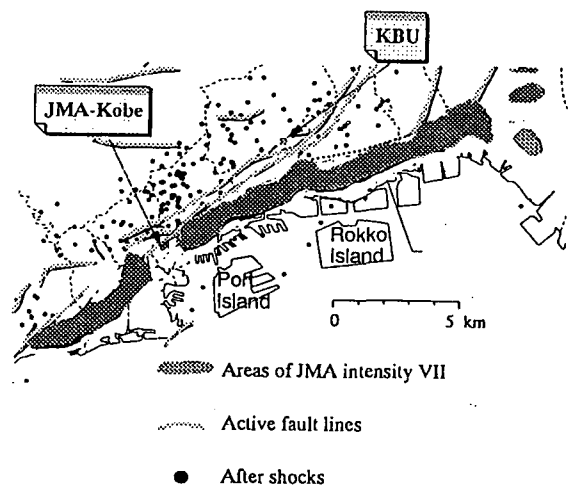

Fig.1 Seismic damage caused by the Hyogo-ken Nanbu Earthquake, 1995.

extremely damaged areas were scattered in spots. These spots are distributed on fluvial plains, buried valleys, and alluvium fans[3]. It is noted that the disaster belt zone was located mainly in the region with relatively thin soft sediments, typically less than 10m in thickness which was contradictory to

the conventional understanding that the seismic damage is severer in the deeper soft soil. Therefore, the local geology and topography might be attributable to the abov disaster belt zone.

This paper gives detailed unified interpretation that focuses the amplification of surface alluvium and underlying deep diluvium and the Osaka Group layers, showing the respective wave field in the two-dimensional modeling. The point of investigation is to clarify the difference of these effects with respect to the period range of motions.

2. OBSERVED GROUND MOTIONS

The central Kobe area, stretching along the foot of the steep Rokko Mountains in the east-west direction, is situated on the alluvia which were accumulated on diluvia, both of which were brought by running river water, but the diluvia brought by extraordinary floods are much stiffer than the former. The diluvia are underlain by the sedimentary Osaka Group layers formed in the era of Pleistocene and then by granite rocks. In view of the geological map[4], the rock formation indicates steep dipping at the foot of the Rokko ranges due to the fault lines running along them. The depth of the surface alluvium, on the other hand, increases by 1 to 2 % gradient in average as the focus moves from the Mountains toward the Inland Sea. The depth of the alluvium along the shoreline is around 20 m or more. **Fig.2** depicts a rough sketch of the topography in the north-south direction, that may be enough to grasp the overall response features in the concerned Kobe area in average.

During the main shock, the earthquake motions were recorded at several locations by the Meteorological Agency, the Kansai Kyogikai, the Japan Railway Company, and other public and private sectors. The Kobe Marine Meteorological Observatory (JMA-Kobe) and Kobe University basement (KBU) records are taken as the representatives. The JMA-Kobe site is not located in the belt zone of JMA intensity VII but on the upper subgroup of the Osaka Group formation close to it. The ground motions in the belt zone should be expected larger than that at JMA-Kobe. Those seismic records indicate very impulsive motions characterized by two high peaks at the beginning of the time history, followed by fluctuations of smaller peaks which are supposed to be affected by the local soil conditions. The Fourier transforms of the NS components are depicted in **Fig. 3** to show their period contents[5].The record at KBU, supposedly indicating the motion on the

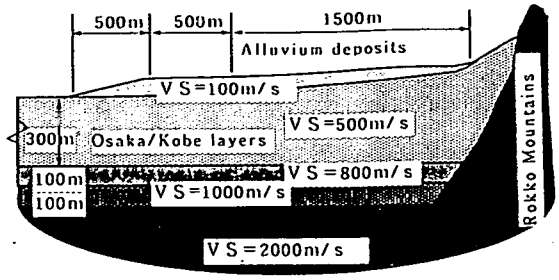

Fig.2 Typical vertical topography of the underground structure in the Kobe area.

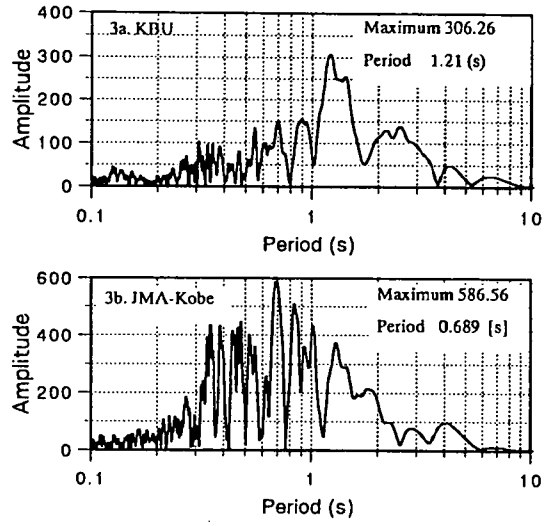

Fig.3 Fourier transforms of the Earthquake records.

rock, has a predominant period of 1.2 second, while the JMA-Kobe record shifts the predominant period toward the shorter range less than 1.0 s.

Immediately after the main shock an array observation of the aftershocks has been done in Kobe area by Iwata *et al* [6]. The observation included a rock site in Rokko Mountains, a stiff soil site near it and alluvium sites in severely damaged zone and slightly damaged area. The spectral ratios from acceleration records at representative observation sites against the rock site revealed the local site effect. The strong peaks appeared in the frequency range of 1.5-3.5 Hz with amplification ratio of more than 40 at the severely damaged location. This indicates the soil resonance at the site. However, the location near the coast with thicker soft soil deposit showed amplification ratio lower than the above in the same frequency range. The peaks in the frequency range less than 1 Hz were almost the same at alluvium sites while the

corresponding values at the stiff soil site near mountain were relatively smaller[6].

The seismic wave reflection survey that was also carried out after the main shock, showed that the existence of active faults beneath Kobe city was not the direct cause of the disaster belt zone formation[7]. However, through this investigation, the deep soil sediments were detected along the measurement lines. The granite rock formation indicates more abrupt dipping down to 1000 - 2000 m, deeper than expected at the foot of Rokko range, then bends to make almost a horizontal level toward Osaka Bay. The stiff diluvium and the Osaka Group soils are deeply deposited on it. Therefore, the geologists pointed out that this deep soil structure might be related to the devastating seismic waves, in contrary to the geotechnical engineers who pay attention to the surface soil amplification effect.

3. SIMULATION OF SITE RESPONSE

The distribution of the ground motions from the foot of Rokko ranges to the coast in the north-south direction is the main interest herein. In view of the topography effect on seismic wave propagation, the stiff deep soil called the Osaka group layers and the surface soft alluvium are separately considered by taking different models. In both models, the surrounding stiff soil or rocks should be taken into account as a far field extent for the focused domain. The computer simulation is conducted by employing the two dimensional time domain FEM-BEM hybrid technique. The irregular soils of interest are modeled by the four nodes finite elements while the surrounding uniform half-space is modeled by the boundary elements. The boundary elements are assumed to have constant values within elements for displacement and traction and their stepwise variation with time increments[8]. The discretization is made to fulfill all the considered wavelengths. Only vertical seismic wave incidence is assumed in what follows.

(1) Deep soil model

In view of the abrupt dipping of the rock formation at the foot of the Rokko range, the wave propagation is focused in the deep Osaka group layers on it. **Fig.4** shows the FEM-BEM model for the computer simulation to represent a section in the NS direction. The dimensions of the model and the material properties are assumed as shown in the figure by referring to the available related information, although size of the model is subjected to the computer capacity used. The material damping is

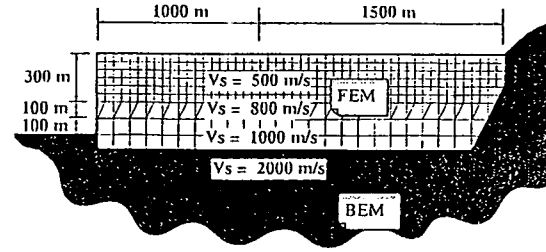

Fig.4 Deep soil model for FEM-BEM analysis.

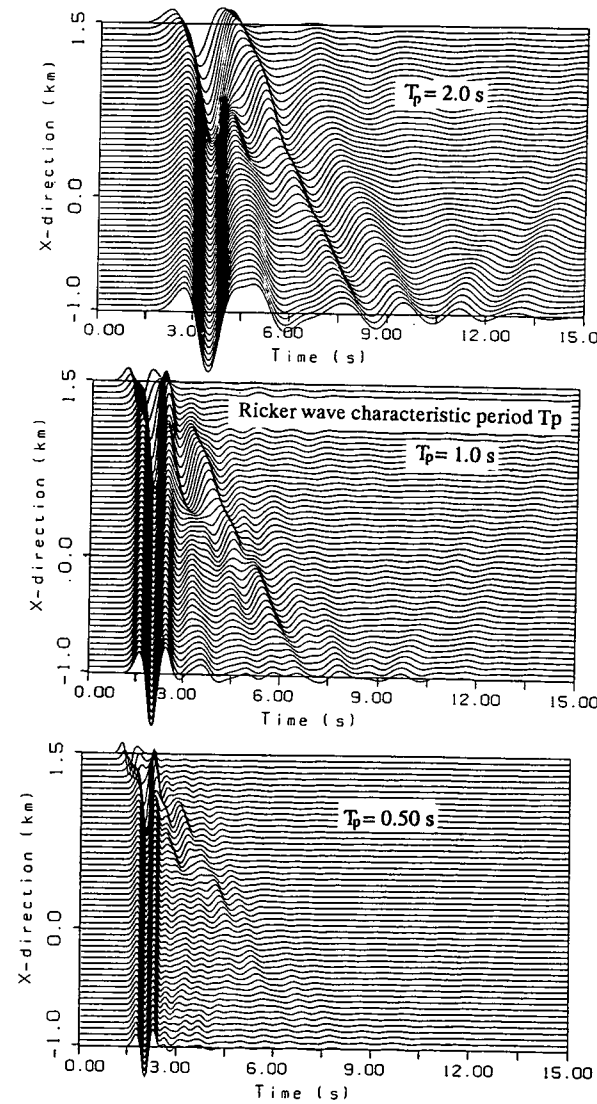

Fig.5 Displacement time histories due to SH-waves.

assigned to the finite element domain as small to 3% in the so-called Rayleigh type because of small strain level in the stiff deep soils. The SH-wave incidence was first presumed to investigate the response features. In order to make clear the

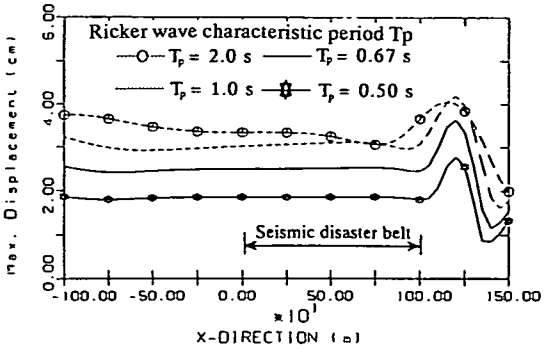

Fig.6 Maximum displacements due to SH-waves.

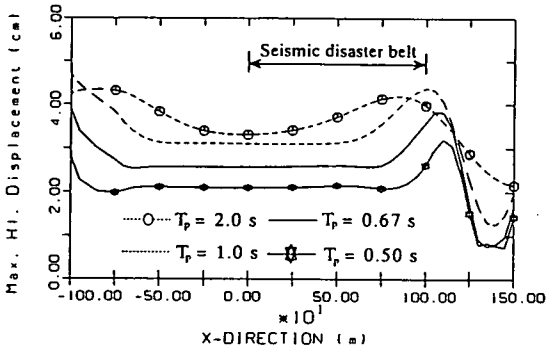

Fig.7 Maximum horizontal displacements due to SV-waves. Ricker wave characteristic period Tp

difference of incident waves in period contents, Ricker wavelets of various characteristic periods (T_p = 0.5 - 2 s) are assumed. The maximum displacement is set to 1 cm for all the computation. The time histories of displacement response are depicted in **Fig.5**. The waves that propagate in the stiff rock arrive at the surface earlier than those that pass through the less stiff Osaka group layers. The abrupt dipping edge generates scattering surface waves that propagate horizontally toward the coast. Those waves come across the vertically propagating waves with low speed in the Osaka group layers as clearly observed in case of T_p = 2.0 s. The amplification due to such wave interference is localized to the vicinity of the abrupt dipping. The maximum displacements along the surface are shown in **Fig.6** for the Ricker wavelets of different characteristic periods T_p. The topography effect on seismic waves is noted to be most significant for the long period input motions in the range of 1 to 2 seconds.

In case of SV-wave incidence, for the sake of numerical computation, the boundary is closed on the coast side at 1000 m far from the area of interest so as to exclude any fictitious side effect on the results. Regarding wave propagation trend,

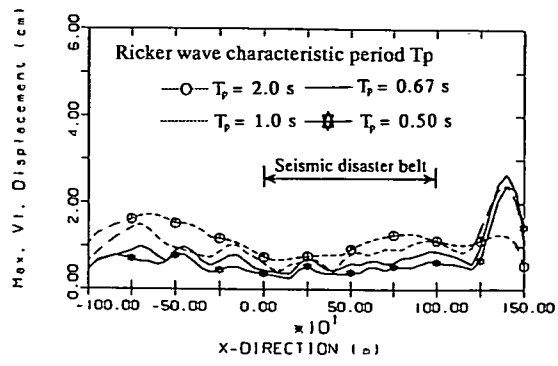

Fig.8 Maximum vertical displacements due to SV-waves.

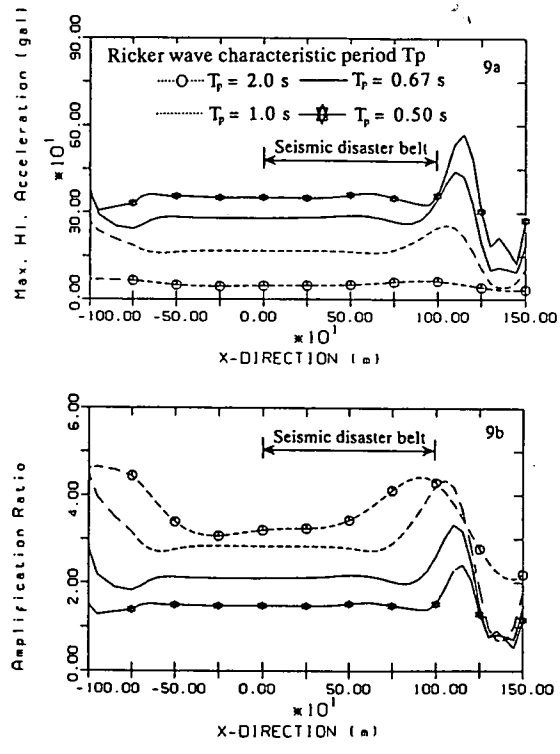

Fig.9 Maximum horizontal accelerations due to SV-waves.

the same behavior as that for the HS-wave incidence is observed. **Fig.7** gives the resulting maximum amplitude of the horizontal displacements. In comparison with the SH-wave responses in **Fig.6**, it is noted that the amplification for the horizontal components is shifted a little away from the mountain side but still confined in a certain limited distance of 500-1000 m from the rock dipping. This is attributable to the different timing of wave interference caused by the different wave velocities of the Love wave (SH-wave case) and the Rayleigh (SV-wave case) wave. The vertical

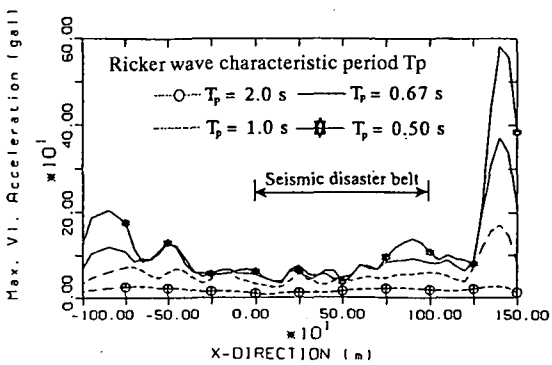

Fig.10 Maximum vertical accelerations due to SV-waves.

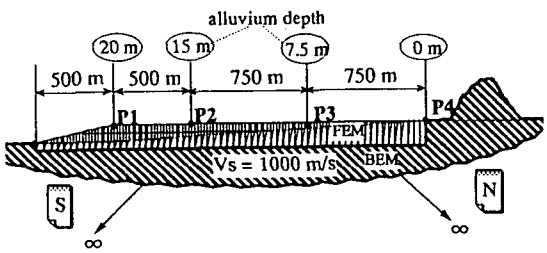

Fig.11 Surface soil model for FEM-BEM analysis.

components for the case of vertical SV incidence resulted mainly due to the wave scattering by the basin edge, whose maximum values were thus concentrated closer to the abrupt dipping location as shown in **Fig.8**.

Fig.9a shows the maximum horizontal accelerations due to the SV-wave incidence. The trend of localized amplification is the same as for the displacements but the maximum amplitudes are reversed in order with respect to the assumed characteristic period T_p. The shorter the incident wave period, the higher the amplitude of the acceleration. This is due to the fact that the same unit amplitude is used for the incident displacement while the acceleration is inversely proportional to the period squared. For instance, for T_p = 2 s, the maximum input acceleration of 14.8 gal results in the maximum horizontal response of 70 gal while, for T_p = 0.5 s, the input of 237 gal leads to the response of 590 gal. The amplification ratio of the surface horizontal acceleration with respect to a unit input is given in **Fig.9b.** The amplification ratio attains the biggest value at T_p = 2 s, indicating around 4 and it becomes less for shorter periods with the smallest value at T_p = 0.5 s. At far distance beyond this amplified zone the amplification ratio remains almost constant values that can be predicted by the one dimensional shear wave propagation theory. It must be mentioned here that the disaster belt of JMA intensity VII is located above this flat zone and the higher amplification ratio is expected, especially in the short period range. Therefore, the deep soil amplification may not be primarily concerned with the heavy damage distribution in the belt zone. The unexpected high amplification at the area near the shoreline (x = -750 to -1000 m) resulted by the wave reflection at the closed boundary employed. But these waves have no effects on the response of the above damage belt zone where our main interest is placed on.

The vertical acceleration responses in **Fig.10** are shifted toward the dipping location of the rock, showing sharp peaks over a narrow area. The short period wave incidence of T_p = 0.5 s attains the highest amplitude whereas the long period wave incidence T_p = 2 s has the smallest value. Interesting to note is that the vertical components in this amplified zone are larger than the horizontal ones for all the periods computed here. Similar behavior is pointed out by others[9].

(2) Surface soil model

In view of the gradually increasing depth of the soft alluvium on which Kobe city directly stands, a uniform wedge-shaped model is assumed for simplicity. **Fig.11** gives the corresponding FEM-BEM model. The dimensions and sharp contrast of soil stiffness are based on the available geological data of Kobe area[10]. Concerning the surrounding soil stiffness, trial cases have been performed to check the sensitivity of this stiffness contrast on the surface response. It was found that the maximum value for all responses was increased in the range of 10 - 15% when the shear wave velocity V_S was increased from 500 to 1000 m/s, indicating the same response profile and the wave propagation along the surface. Therefore, only the results for the V_S=1000 m/s as a mean value in the far field due to SV-wave incidence will be presented herein. The above stiffness contrast may be tempting to analyze the response of a surface layer by employing the one dimensional wave theory. However, the interface configuration of sharp edges with the surrounding half-space is important since it generates surface waves that leads a very complex wave field together with the vertically propagating body waves.

The damping ratio of 3 % is assumed also for the finite element domain for the alluvium. This ratio may not be enough for the analysis of such soft soil

layer, especially when it is subjected to high strain levels. But in view of the big amplification of the surface alluvium, a high damping should not be assigned to the soil layer for interpreting the heavy damage belt zone. Also, a small damping is convenient to investigate the characteristics of the site response and the generation of surface wave by the topography. The Ricker wavelets of various characteristic periods (T_p = 0.5 - 2s) are used as incident SV-wave at the far field. The above mentioned periods correspond to the incident wavelengths between 500 and 2000 m at the site. The so-called dimensionless frequency that is defined as the ratio between the surface width of the concerned topography and the incident wavelength varies between 1.25 and 5. According to the previous studies[8], these values may have a substantial influence of the topography on the seismic wave propagation in the assumed model.

Fig.12 shows the time histories of the surface horizontal displacements. For a long period input motion (T_p = 2 s) the response appears in the same form as the input motion but is doubled in amplitudes and no horizontal surface wave propagation just like the response for a uniform half-space (**Fig.12a**). For shorter period input motions (T_p = 1, 0.67, 0.5 s), we notice that surface waves start to emerge from different locations on the surface and propagate horizontally, (**Fig.12b, c, d**). As the period becomes shorter, the location of such wave generation moves nearer to the sharp edge. The higher response and the longer duration can be clearly observed. The same wave propagation phenomena has been seen for the velocity and acceleration which are omitted here. **Fig.13** depicts the maximum displacements and accelerations along the surface of the alluvium. The higher response can be clearly observed for shorter period motions in the wide area including the disaster belt zone. For a shorter period input, the location of the maximum value is shifted toward the sharp edge of the alluvium (at the foot of Rokko Mountain). Concerning the structural heavy damage in the disaster belt zone, the highest responses are evidently involved in it. Therefore, we can conclude that the critical period for this area lies between 0.5 and 0.8 second. This period range coincides with the fundamental periods of the most heavily damaged structures in the disaster belt zone.

The above response features may be explained as follows from the wave propagation mechanism: A Ricker wavelet has the major spectral densities around the characteristic period. The predominant period of a soil layer, although the two-dimensional motions have more complicated period contents, is

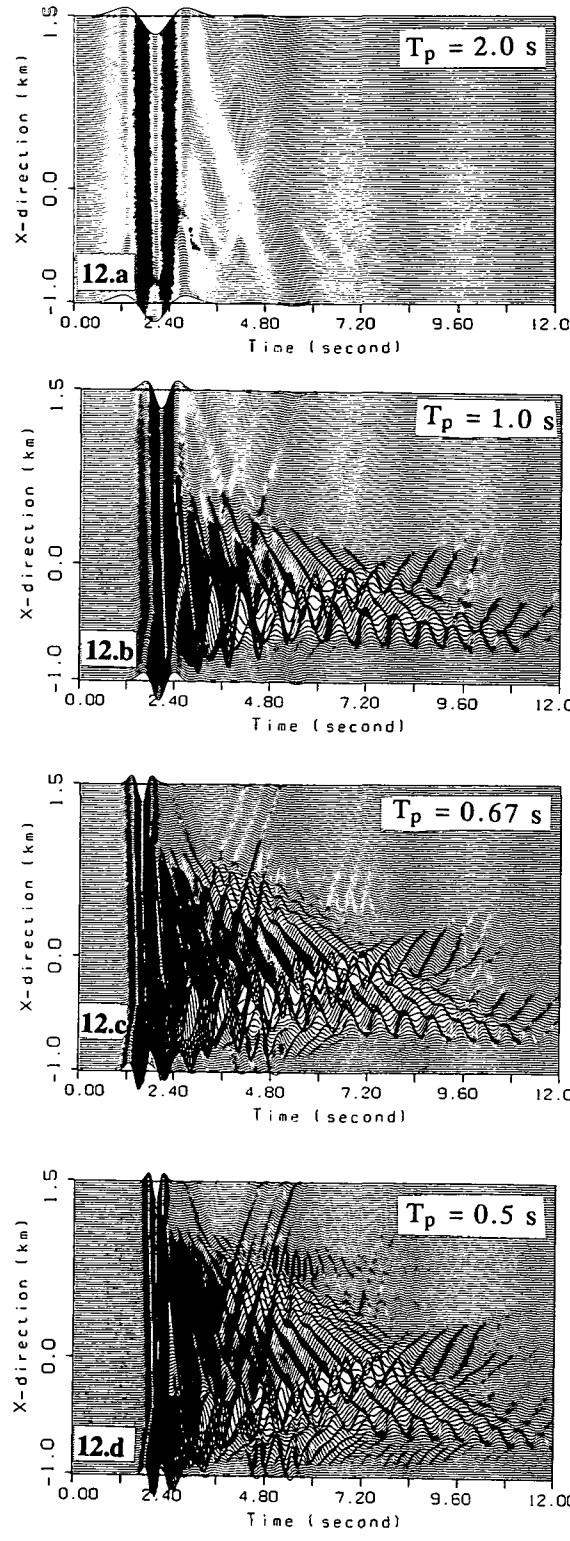

Fig.12 Alluvium surface displacement time histories due to SV-Ricker waves (horizontal components).

estimated by the formula $T_p = 4H/V_S$ (H= alluvium depth, V_S= shear wave velocity) based on the one dimensional model. This leads to a phenomenon that specific soil locations can come into resonance at the respective characteristic periods, thus, it enables surface waves to emerge and propagate horizontally. Suppose that the first incident wavelet is followed by another one traveling vertically so that the interference occurs between the horizontally propagating surface waves and those traveling vertically in the alluvium. This interference results in longer duration, highly amplified responses and may cause succeeding resonance of other portions of the surface layer. This mechanism, which we call it "bump effect"[5], can not be explained by the one-dimensional wave analysis.

In order to investigate the wave interference more clearly, we take two types of artificial input motions: long period motion (predominant period longer than 1 second) and the short period motion (predominant period shorter than 1 second). These artificial earthquake-like motions are approximated by a set of five Ricker wavelets so as to attain the required period contents[5] and scaled to give the same maximum input acceleration for the both. The acceleration time histories and the period contents of these motions are given in **Fig.14a** and **Fig.14b**, respectively. The associated horizontal displacement time histories of the soil surface are shown in **Fig.15a** and **Fig.15b**. The interference between the horizontally and vertically propagating waves is obviously observed in the case of short period input motions. The maximum responses are centered in the disaster belt zone and appear after the third peak of the input motion arrived at the surface when the constructive wave interference are taking place. Except for the resonance phenomena near the shoreline, the long period input motion induced no surface wave generation so that no high response amplification results.

Next, the more complicated simulation was carried out. The vertical incidence of SV-wave is assumed for the NS directional motions. Selection of a seismic record at a site as an input motion to another site should be done carefully for the better prediction of the latter. Suppose the KBU record is obtained at the outcropping rock site, then one half of its amplitude may be taken as an input motion in the far field. The most important portion of the computed displacements (12 seconds in duration) are chosen for the computation. Another possible choice of the input motion may be the deconvoluted motion to the alluvium base for the JMA-Kobe surface motion. The one dimensional procedure was carried out for this purpose and

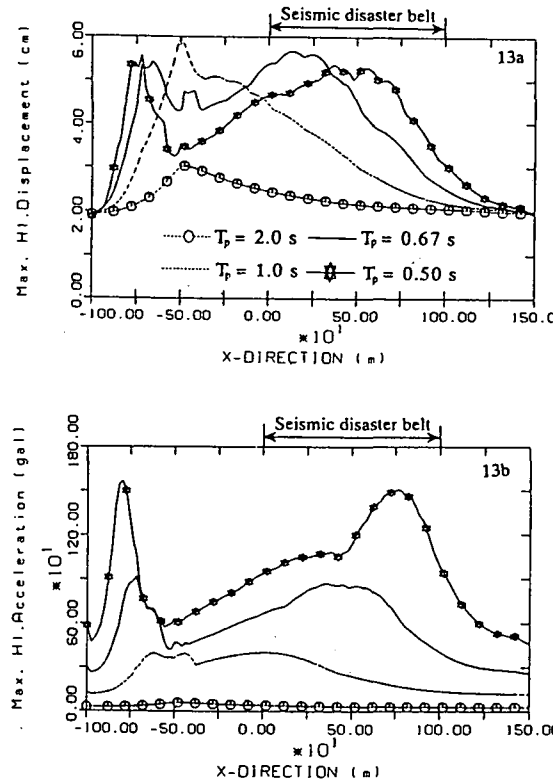

Fig.13 Alluvium surface maximum responses due to SV-Ricker wavelets (horizontal components).

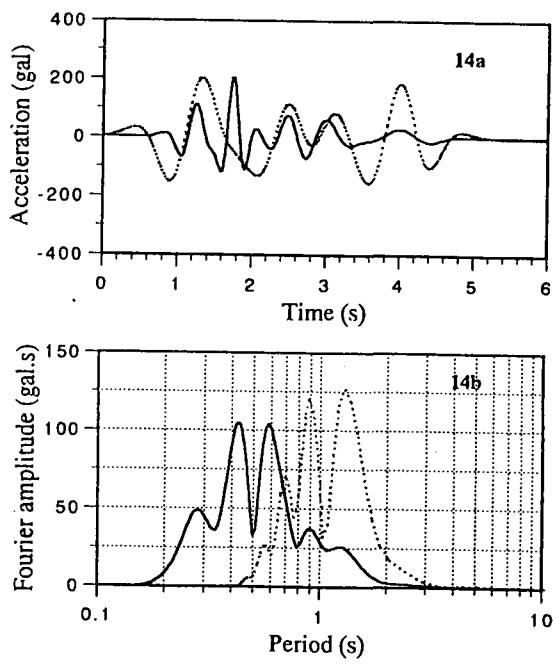

Fig.14 Acceleration time histories and period contents of the artificial input motions.

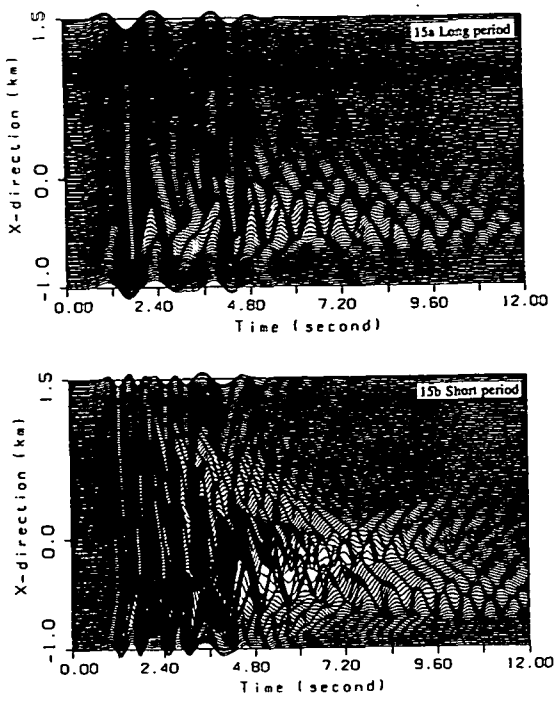

Fig.15 Horizontal displacement time histories due the artificial long and short period input motions.

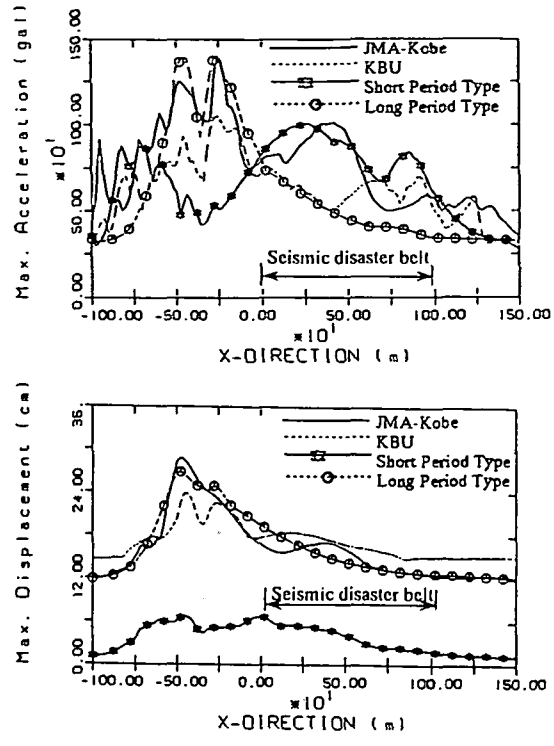

Fig.17 Alluvium surface maximum responses due to different input motions (horizontal component)

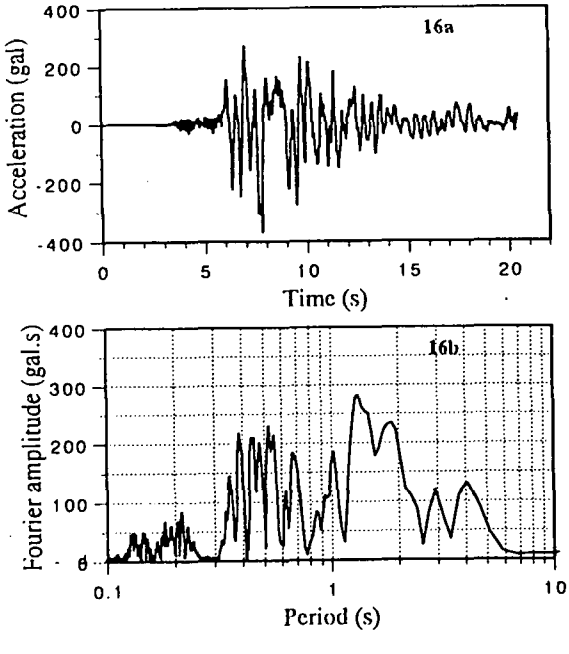

Fig.16 Acceleration time history and period contents of the deconvoluted JMA-Kobe NS component

the resulting motion was used for the two-dimensional analysis of the alluvium. The acceleration time history that showed the peek value of about 360 gal is depicted in **Fig.16a**. The period contents of this acceleration (**Fig.16b**) indicates comparable amplitudes to those of the KBU record in the long period range but also with substantial amplitudes in the short period range.

The maximum horizontal response profiles due to different input motions are shown in **Fig.17**. For the KBU record as an input motion, the large acceleration amplification appears in the area closer to the shoreline and a moderate amplification near the foot of the Rokko range. There is no high acceleration amplification in the seismic disaster belt zone. Since the surface acceleration is related to the seismic force action to structures on the ground, it may be stated that the KBU records, affected by the local site conditions and amplified at the long period motion in the range longer than 1 second, can not explain the heavy damages in the disaster belt zone. The deconvoluted JMA-Kobe input motion, on the other hand, yields the maximum acceleration response distribution with higher response in the heavy damage belt zone and the peak ground

accelerations closer to the shoreline. The latter high accelerations were not evident during the main event because of the sever nonlinear soil behavior and/or liquefaction phenomena occurred along the shoreline which were not considered in the present analysis. Thus, we limit our discussion to the linear behavior in the belt zone and the nonlinear behavior is investigated and stated in our next publication[11].

The maximum response profiles due to the two types of artificial input motions are also given in **Fig.17** for comparison. It is noted that the long period motions are related to the displacement whereas the short period motions are concerned with the acceleration at the disaster belt zone. The small displacement in the case of the short period type input motion is due to the adjustment that the maximum input displacement is set to 0.60 cm while for the long period type to 3.90 cm to give rise to the same maximum input accelerations. At least to explain the strong acceleration amplification at the heavy damage belt zone, the short period type motions may be pointed out. These results confirm our suggestion for the critical periods and wave propagation characteristics in the seismic disaster belt zone.

The Fourier amplitude ratio between P2 location at the alluvium surface and P4 at the foot of Rokko ranges is shown in **Fig.18** when the KBU motion is used as an input. The sharp amplification is centered at the predominant period of 0.499 s (about 2 Hz frequency) with a maximum ratio of 32. This finding agrees with the aftershock observations stated in section 2[5].

Fig.19 shows the time histories of soil surface acceleration, velocity and displacement responses due to the deconvoluted JMA-Kobe records. Interesting to note is the large displacement of long period motions while the intensive acceleration of short period motions takes place. This soil behavior leads to the worst situation to the aboveground structures when they become in resonance in the acceleration period. The phase difference along the horizontal distance is obvious since the horizontal wave propagation can be noticed. The wave interference occurred between horizontally propagating waves and the those propagating vertically along the alluvium depth.

4. CONCLUSIONS

In this paper, in order to better understand the site effects during the Hyogo-ken Nanbu Earthquake, 1995, two separate models are taken for the soil structure for the computer simulation:

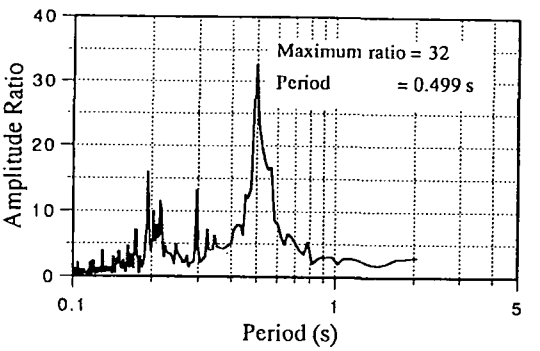

Fig.18 Fourier amplitude ratio between location P2 and P4 (see **Fig.11**).

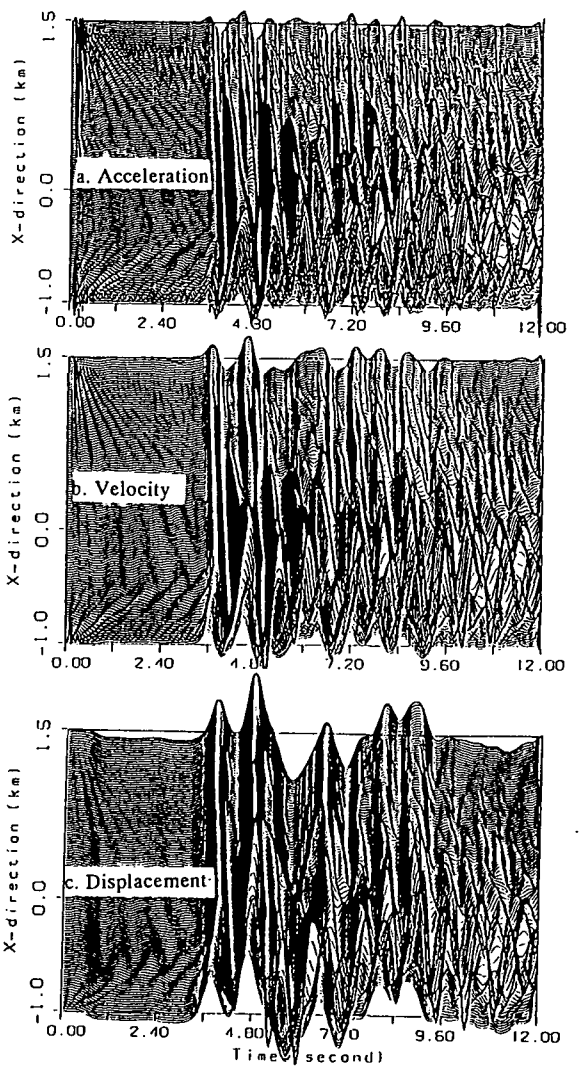

Fig.19 Alluvium surface maximum response time histories due to JMA-Kobe input motion

The deep soil model to describe the dipping of the rock formation on which the Osaka group layers lie and the shallow soil model to describe the wedge-shaped surface soft alluvium. The results revealed the relevant wave propagation mechanism in the irregular topography at Kobe, which can explain rationally the observed heavy damage.

From the analysis of the deep soil model, we state that the abrupt dipping of the rock formation causes the wave scattering that leads to the seismic wave amplification near this dipping. Under the assumption of the SH-and SV-wave incidence the horizontal responses are significantly amplified in the period range of 1 to 2 s in a limited extent of 500-1000 m from the edge. The vertical response amplification, on the other hand, occurs closer location to this dipping at the short period motions around 0.5 s. Noteworthy is that the latter component exceeds the former in this region.

From the analysis of the surface soil model, we note that the gradually increasing alluvium amplifies the seismic waves in the period range shorter than 1 second. The wave interferences between the horizontally propagating waves and the vertically propagating waves lead to the amplification of seismic waves at the location that coincides with the disaster belt zone. The computed maximum responses for the deconvoluted motion of the JMA-Kobe record correspond well with the heaviness of the observed seismic damage.

Based on these results, we conclude that the deep soil sedimentation might have had contribution to the response amplification in the long period motions away from the disaster belt zone, while the shallow depth alluvium might be most concerned with heavy damage distribution at Kobe during the Hyogo-ken Nanbu Earthquake.

REFERENCES

1) Japan Society of Civil Engineers: Report on the Great Hanshin Earthquake Disaster, 1995.2.
2) Kohketsu, K.: Are predominant period contents of strong motions the major cause of sever damage by the Kobe earthquake?, *Monthly Journal of Science, Kagaku Asahi*, No. 652, pp.11-14, 1995.
3) Ishikawa, K., Mizoguchi, S. and Ono, S.: Gelology of Kobe Area and Earthquake disaster Zone, *Proceedings.of Symp. on the Hanshin-Awaji Great Disaster*, JSCE, pp.187-194, 1996 (in Japanese).
4) URBAN KUBOTA 30, Kubota, March 1995.
5) Takemiya, H. and Adam, M.: Why the heaviest damages occurred in Kobe during the Hyogo-ken Nanbu Earthquake, Japan 1995, *The Kobe Earthquake: Geodynamical aspect*,, edited by Brebbia, C.A., Computational Mechanics Publication, Southampton, UK, pp.39-58, 1995.
6) Iwata T., Hatayama, K., Kawase, H., Irikura, K. and Matsunami, K.: Array observation of aftershocks of the 1995 Hyogoken-nambu earthquake at Higashinada Ward, Kobe City, J. Natural Disast. Sci., Vol.16, No.2, pp.41-48, 1995.
7) Ito, S., Yokota, H. and Watanabe, T.: On ground structure and earthquake motions of Mt. Rokko foothill area based on seismic survey results, *Proceedings of Symp. on the Great Hnashin-Awaji disaster*, Osaka City University, Session No. VI, 1996.
8) Takemiya, H., Adam, M. and Yasui, S.: Transient seismic response of irregular sites, *Proceedings of the 3rd Int. Conf. on Recent Advances in Geotechnical Earthq. Eng. and Soil Dynamics*. St. Louis, MO USA, 1995.
9) Kawase, H.: Strong motion simulation in Sannomiya, Kobe, during the 1995 Hyogo-ken Nambu earthquake considering nonlinear response of shallow soil layers, *Proc. of the International Workshop on Site Response subjected to Strong Earthquake Motions*, Yokosuka, Japan, Jan. 16-17, 2, pp.171-184, 1996.
10) Kobe City Office: Ground condition in Kobe (Kobe no Jiban), Kobe, Japan, 1980 (in Japanese).
11) Takemiya, H. and Adam, M.: Nonlinear soil behavior in Kobe during the Hyogo-ken Nanabu Earthquake, submitted to JSCE for publication.

(Received June 6, 1996)

兵庫県南部地震における神戸の地形・地質による地震波の増幅

竹宮宏和・アダム マヘール

兵庫県南部地震(1995.1.17)は内陸型の活断層によるもので，気象庁震度階VIIの震災の帯を神戸に生じさせた．本論文では，神戸の地質・地形の特徴，つまり，六甲山麓の断層による基盤岩の急激な落差，海岸に向かって深さの漸増する沖積層に注目して，この現象をコンピューターシミュレーションから究明した．その結果，前者の影響は短周期成分(0.5～1秒)で，後者は長周期成分(1～2秒)で顕著であること，そしてそれぞれによる地震波の増幅場所から震災の帯の形成にはより前者が関係したと結論している．